SSRG International Journal of Mechanical Engineering
ISSN: 2348-8360/ https://doi.org/10.14445/23488360/IJME-V11I6P103

Volume 11 Issue 6, 19-26, June 2024

Original Article

Investigating the Enhancement of Mechanical Properties through Hardfacing in Submerged Arc Welding: An Experimental Approach

Yogesh Agrawal[1*], Anil Singh Yadav[2], Nitin Tenguria[3], Santosh Katkade[1], Abhishek Sharma[4]

[1]*Mechanical Engineering Department, Sandip Institute of Technology and Research Centre, Nashik, Maharashtra, India.*
[2]*Mechanical Engineering Department, Bakhtiyarpur College of Engineering (Science, Technology and Technical Education Department, Govt. of Bihar), Bakhtiyarpur, Patna, Bihar, India.*
[3]*Mechanical Engineering Department, Sagar Institute of Research and Technology-Excellence, Bhopal, MP, India.*
[4]*Mechanical Engineering Department, B I T Sindri, Dhanbad, Jharkhand, India.*

[1]*Corresponding Author : a80yogi@gmail.com*

Received: 03 April 2024 Revised: 15 May 2024 Accepted: 07 June 2024 Published: 30 June 2024

***Abstract** - Hard facing is a surfacing technique in which a hard layer is deposited over soft material to improve wear resistance. In this article iron based hard facing has been successfully developed with the help of submerged arc welding. Since iron-based alloy associates with low cost and better metallurgical properties, it has been chosen for the final experiment in this work. Three hard-facing layers with different carbon content have been successfully developed without any defects. The mechanical and metallurgical characteristics of the created hard facing alloy have been examined, and it displayed a substantial increase in properties over the basic material. Microstructures of the deposited layer exhibit a combination of hard carbides and austenite, with carbides embedded in a soft austenite matrix. As the quantity of alloying elements increases, the microstructure likewise exhibits an increase in carbide volume percentage. The hardness of the hard-facing layer has also improved by 142.5% as compared to the base material, and it is improving as the carbon and chromium percentages increase. Erosive wear study showed improvement in erosion resistance of deposited layer as compared to base material and resistance to erosion is increasing with increment of carbon percentages more amount of carbon produces more volume of carbides.*

***Keywords** - Erosive wear, Fe-Cr-C, Hardness, Submerged arc welding, Wear resistance.*

1. Introduction

Wear is the continuous or gradual degradation of any metal caused by misuse via material loss. It causes preformation loss owing to deterioration in part condition. Wear has the potential to diminish lifespan and productivity. Wearing may put workers in danger. Wear might result in increased energy use and reduced yield. Metal filler in the forms of hotwire and powder may be utilized in this process. Two systems work together in plasma arc surfacing, one to melt the wire and lay it over the base metal and the other to hold the plasma torch to melt the base metal and fuse them. This method results in little base metal diluting or distorting and a great quality surface with minimal polishing. Hotwire must constantly be in touch with base metal; hence, this technology is only practical in automated mode and at a high cost. The hard-facing material is deposited at a high temperature of between 5,500 °C and 22,000 °C. This method of metal deposition results in deposits that are homogeneous and fully fused with the base metal, ensuring a high-quality and well-fused metallurgical structure. These machines are somewhat pricey, but they can deposit a variety of hard facing materials. The deposit thickness and surface smoothness may be precisely controlled using this method. The benefits of the submerged arc surfacing technology have made it the de facto standard. The result is a very rapid rate of deposit. High quality, high strength, toughness, or abrasion resistance may be achieved with this deposition method. While the flux shields the bead from damage, more dilution may occur if the flux has to penetrate deeply [1-6]. Chang et al. [7] have experience using GTAW on top of a hard-facing alloy composed of Fe, Cr, and C. The substrate was made of ASTM A36 steel, while the filler was a chromium and graphite alloy. The microstructure of the Fe-Cr phase and [$(Fe\text{-}Cr)_7 C_3$] carbide changes when authors incorporate different types of graphite. As the percentage of primary [$(Fe\text{-}Cr)_7 C_3$] carbide in the hard-facing alloy grows, so does the alloy's hardness. The results of an abrasive wear test show that primary [$(Fe\text{-}Cr)_7 C_3$] carbide is superior to quartz in terms of wear resistance because its hardness is significantly greater than that of quartz (about 1600HV against 1000-1100HV). The addition of modest amounts of carbon resulted in continuous scratches, but an increase in carbon and primary [$(Fe\text{-}Cr)_7$ C_3] carbide led to the production of discontinuous scratches and an increase in crater formation. As a result, when graphite is included in the Fe-Cr-C alloy, the development of tough [$(Fe\text{-}Cr)_7$ C_3] carbides is encouraged. The wear test results show that the alloy is resistant to abrasion because hard carbides develop throughout the process. For the cladding procedure, Chen et al. [8] utilized gas tungsten arc welding using a Fe-CrC hard-facing alloy. Deposited as a hard-facing alloy on low Carbon Steel, commercially pure Fe of varying Cr-C composition is utilized as a filler metal. The dimensions of the sample were 100 mm x 40 mm x 10 mm.

The experiment's filler was made from a powder combination including varying amounts of Fe and Cr-C, with the goal of achieving a wide range of possible microstructures for the hard-facing alloy system. After the experiment was completed, the hard face layer's chemical composition was analysed using an optical emission spectrograph. Microstructures were seen using optical and scanning electron microscopy. The structural phases were determined by X-ray diffraction analysis. The tests revealed a variety of microstructures. Hypoeutectic, near-eutectic, and hypereutectic structures were identified as developing with increasing Cr-C levels. Primary -Fe phase was used to create the hypoeutectic structure, whereas primary [$(Fe\text{-}Cr)_7$ C_3] carbide was used to create the hypereutectic structure. The hypoeutectic microstructure, thus, has a softer hardness than other microstructures.

The research by Morsy and El-Kashif [9] was conducted on a mild steel Hard-facing substrate for use with a variety of electrode types. Microstructure obtained from various electrodes using GMAW and MMAW are compared. It requires four electrodes total: two tubular [DIN 8555: E10-GF-60GR1 and E10-GF-60GR2] and two covered [A and B] [DIN 8555: E6-UM-60 and E10-UM-60GR]. In order to infer the wear resistance of the deposit layers, XRD must first be performed on this electrode. Hard face is applied to a mild steel (10 mm) substrate utilizing covered and tubular electrodes in a Metal Arc Welding (MMAW) technique. Substrate hardness and microstructure are then evaluated. Pin-on-disc abrasion tests were performed using a tribometer.

The results of the tests indicate that the electrode, a configuration producing the martensitic microstructure, results in the lowest wear resistance. While electrodes B and C both contain carbon, the wear resistance of electrode C (the tubular one) is higher than that of electrode B (the covered one). Electrode D has greater wear resistance than electrode C while having the same carbide area percentage and hypereutectic structure. Different Iron-based hard-facing alloys were subjected to abrasion testing by Kirchgaßner et al. [10]. Gas metal arc welding was used for research purposes. The authors compared a low alloyed material based on Fe-Cr-B-C alloy to a more complicated alloy containing boron, namely Fe-Cr-W-Mo-Nb. The purpose of this study was to compare the gas metal arc welding wear resistance of six different Fe-based hard-facing alloys. It measures both the abrasive wear and the combined abrasive and impact wear. Substrate was 1.0038 mild steel, and flux cored wires of six distinct Fe-based hard-facing alloys were manufactured.

All welding was done using a 1.6mm wire diameter, and it was done in two layers. Numerous research studies have focused on the experimental investigation of enhancing mechanical properties through hard-facing developed by submerged arc welding, leading to significant improvements in material strength and durability. [11-16].

The wear resistance and outstanding comprehensive properties of Fe-Cr-C hard facings have made them popular in the mineral processing, metallurgy, and mechanical industries. Arc welding is the most common method for creating hard-facing alloys. SMAW is the most well-known kind of arc welding [17-23]. The following goals have been established:

- To develop the iron-based hard-facing layer.
- To investigate the hardness of the hard-faced layer.
- To investigate the wear resistance of the developed hard facings using an erosive wear test rig.

2. Materials and Methods

2.1. Selection of Base Metal

The final experiment's base metal, mild steel, was chosen because of its widespread usage in the manufacturing and construction sectors. Using a power hacksaw, these plates were sized to 280 mm, 50 mm and 12 mm.

The power hacksaw machine is shown in Figure 1 for the processing of plate material. Before welding, acetone was used to remove oil and grease from the plates.

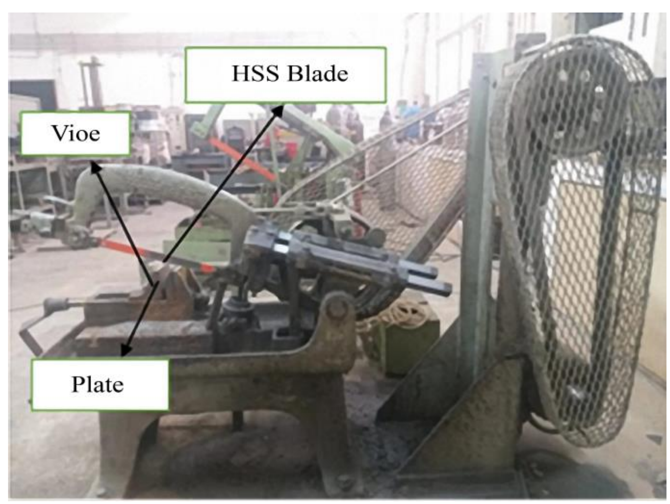

Fig. 1 Power hacksaw

Table 1 shows the foundation material's chemical makeup.

Table 1. Chemical composition of base material

Element	C	Si	Mn	Cr	S
Weight Percentage	0.177	0.161	0.50	0.082	0.036

2.2. Choosing the Right Powder for Hard-Facing

For the purpose of creating a hard-faced layer over the foundation material, the ferro-chrome metal powder was opted for. Fe-Cr powder was chosen because of its inexpensive price and high metallurgical compatibility with other materials.

Some metal powders were utilized in addition to Fe-Cr to improve the deposited layer's properties. Table 2-4 below provides the chemical makeup of metal particles.

Table 2. Fe-Cr metal powder

Element	Cr	C	S	P	Si	Fe
Weight Percentage (%)	72.55	0.067	0.012	0.023	0.68	26.67

Table 3. Fe-Mn metal powder

Element	Mn	C	S	P	Si	Fe
Weight Percentage (%)	84.27	0.72	0.011	0.13	0.91	13.96

Table 4. Fe-Si metal powder

Element	Si	C	S	P	Mn	Fe
Weight Percentage (%)	48.76	0.071	0.02	0.021	0.39	50.74

2.3. Hard Facing Methodology

Paste composed of a predetermined quantity of powder mixed with a silicate binder was sprayed over the substrate. After coating the plates and waiting 24 hours for them to dry, they were roasted at 200 °C to remove any remaining moisture. This metal powder was melted and fixed onto the substrate using a submerged arc welding process.

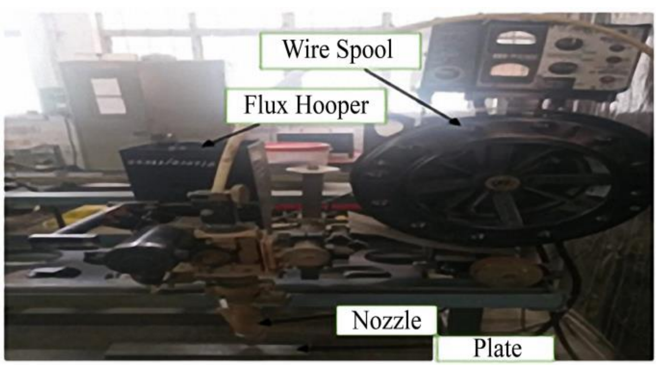

Fig. 2 Submerged arc welding machine

The welding machine's table doubled as a rack for hot plates. Welding was performed using a DC positive electrode shown in Figure 2. The metal powder was melted by creating an arc above the paste. After the surface solidified, the slag was scraped off and hard-facing applied. To prepare the weld bead for the next steps, it was first chipped with a hammer and then cleaned with acetone. Because the appropriate welding conditions and adequate material composition were unknown, an excessive number of faults were seen when trial runs began.

Table 5. The parametric window for the welding process parameter

Current (Amp)	300-550
Voltage(V)	36-50
Speed(mm/s)	4-9
Nozzle to Plate Distance(mm)	15-22
Wire feed(mm/s)	12-18

Table 6. Final welding parameters

Voltage(V)	42
Current (Amp)	400
Speed (mm/s)	4
Nozzle to Plate Distance(mm)	15
Wire feed(mm/s)	12

Welding process parameters are shown in the Table 5-6. Three hard-faced layers with distinct carbon percentages were manufactured by adjusting the graphite proportion on purpose. The purpose of these tests was to examine how changing the carbon content of the finished hard-faced layer affected the product. After completing the hard-faced layer composition development, the plates were sliced into various parts. The welded plates were reduced to size using an abrasive cutter shown in Figure 3 for the various tests. The layer's chemical makeup was the first thing examined. The formation of carbides in the hard-faced layers is a major contributor to the issue; thus, understanding the elemental makeup of these layers is crucial. Optical Emission Spectroscopy (OES) was utilized to analyze the sample for its chemical Makeup.

Fig. 3 Abrasive cutter

The welded plates were reduced to size using an abrasive cutter for the various tests. The layer's chemical makeup was the first thing examined. The formation of carbides in the hard-faced layers is a major contributor to the issue; thus, understanding the elemental makeup of these layers is crucial. Optical Emission Spectroscopy (OES) was utilized to analyze the sample for its chemical makeup shown in Figure 4.

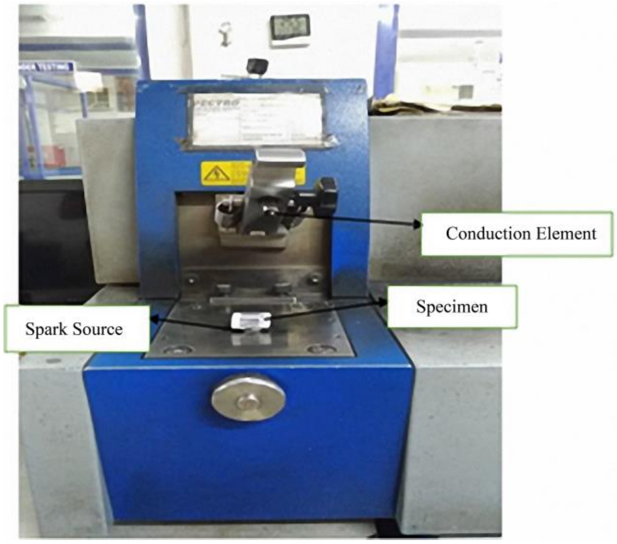

Fig. 4 Optical emission spectroscopy

The sample (10x15mm) is heated to over a thousand degrees by an electrically high voltage source in the spectrometer in an OES analyzer. The sample is heated at its surface as the electrical discharge, generated by the voltage differential between the electrode and the sample, travels through the material. Both arc and spark discharges are possible for electrical discharge. Elemental emission lines are released when the substance vaporizes, and the atoms get excited. Several lines of optical emission have been detected from the plasma pass, also known as a vaporized sample. An appropriate detector measures the intensity of the incoming light at each wavelength after a diffraction grating has separated it into its component wavelengths. The concentration of the offsetting element in the sample is directly correlated to the wavelength's intensity. After that, the linked computer system takes in the intensity readings and runs them through some predetermined calibration to get the concentration of elements. The outcome is presented in a way that makes it easy to print or save for later use.

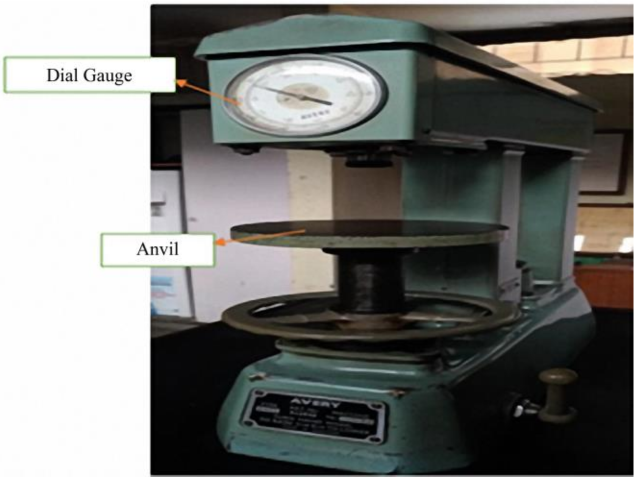

Fig. 5 Hardness test equipment

2.4. The Hardness Test

The hardness test was performed next. The Rockwell hardness tester shown in Figure 5 was used to determine the material's hardness since this instrument provides the bulk hardness that is always necessary for a hard-facing layer. The dimensions of the sample were 10 mm x 15 mm x 12 mm. First, the weld bead surface was polished to remove any imperfections like sink marks, burrs, or other prominence.

2.5. Microstructure Evaluation

The microstructure analysis was performed on a 10x10 mm specimen. The bead surface was appropriately polished after the specimen was cut using an abrasive cutter. The specimen was initially cast in a mold so that it could be polished with little effort. A binder and thermosetting powder were poured into a specimen container and then waited for minutes. To smooth out the top of the weld bead, the authors utilize silicon carbide paper of varying grades. First, a belt grinder was used to polish the specimen using 220-grit paper shown in Figure 6.

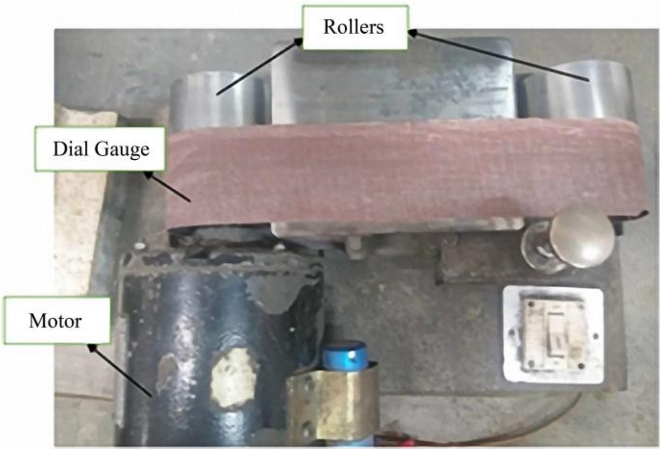

Fig. 6 Belt grinder

Fig. 7 Polishing machine apparatus

The paper grades used next increase from 320 to 400 to 600 to 800 to 1000 to 1200. The semi-automatic polishing equipment with a revolving polishing head is employed shown in Figure 7. The last stage in achieving a high level of polish on the same machine was accomplished using aluminium paste. Etching using a chemical agent follows adequate polishing. After the image has been protected, optical microscopy is utilized to examine the microstructure.

2.6. Erosion Test

A 20x25x5 mm (LxWxT) erosive wear test specimen was used to examine the wear behavior of the hard-faced layer after it had been produced. The specimen's weight was measured before and after an erosive wear test, shown in Figure 8, in which hard particles (Alumina) were impinged on its surface using compressed air. The wear behavior of the hard-faced layer was predicted based on the weight loss computed from the final weight. Table 7 lists the procedure parameters that were employed to account for erosive wear.

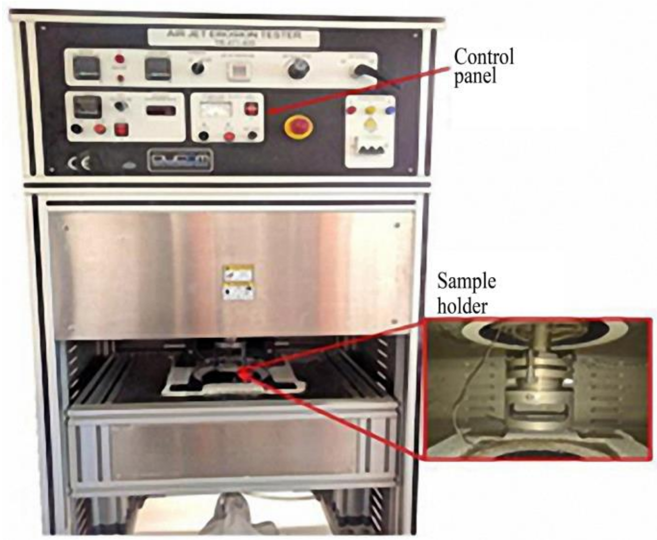

Fig. 8 Erosive wear testing machine

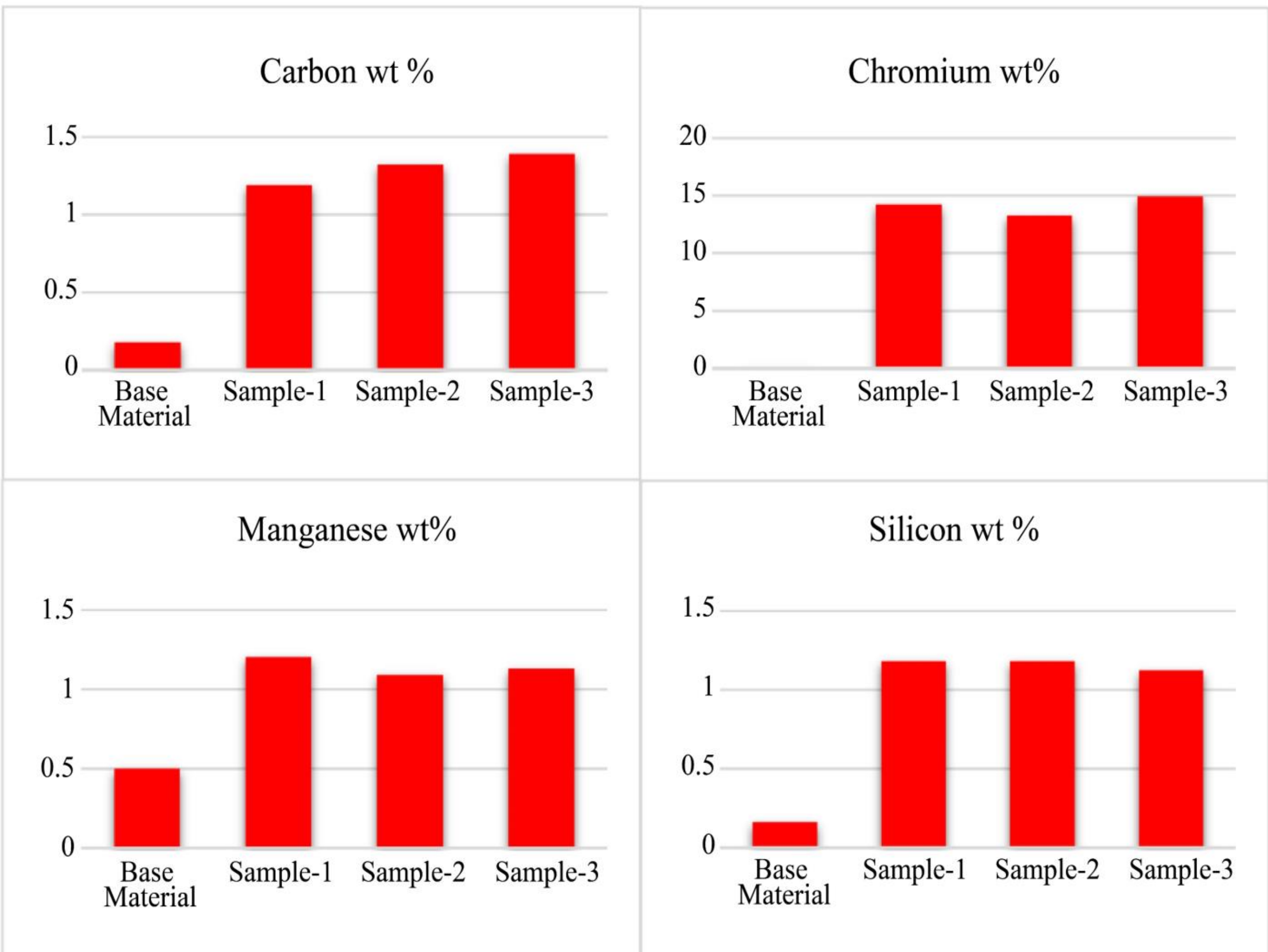

Fig. 9 Distribution of elements in chemical composition

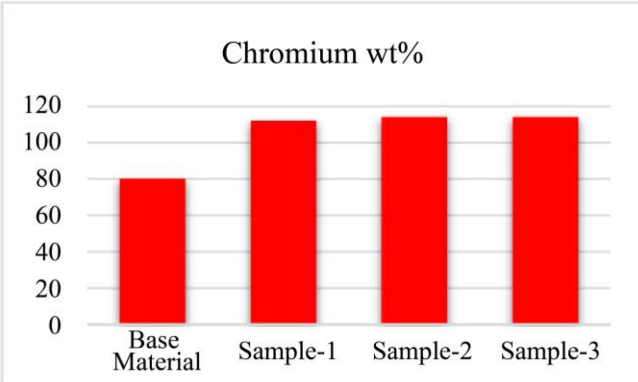

Fig. 10 Hardness comparison

Table 7. Erosion test parameters

Parameters	Particulars
Erodent particle	AI_2O_3
Feed	5gram/minute
Angle of impact	30°
Size of particle	50 microns
Pressure of jet	2.19 bar
Velocity of air jet	70 m/s
Diameter of nozzle	4 mm
Temperature	Room Temperature
Time	30min

3. Results and Discussion

3.1. Chemical Composition Analysis

Analyses of the produced hard-faced layer's chemical composition were performed. The particular emphasis of this research was on the behavior of metal transfers, including Chromium, Carbon, and other elements. Carbon, chromium, manganese, and silicon concentrations in the hard-facing layer are substantially greater than in the base metal according to analysis. This proves that the technique used in this study for producing a hard-faced layer with a high proportion of alloying elements is effective.

According to the analysis, the carbon content of the paste increases with increasing graphite percentages. However, the rate of increase in carbon content slackens down significantly after that. Above a certain percentage, the hard-faced layer formed by graphite's strong thermal conductivity absorbs more heat and transmits less to the base metal.

3.2. Hardness Analysis

Each sample was subjected to a hardness test at 10 Kg load to verify the reported hardness value. The produced hard-faced layer and the base metal both have hardness values. The HRB scale was used to measure the hardness of the base material. The hardness value of the hard-faced layer rises as the percentage of alloying is done, as seen in Figure 9.

Although the increase in carbon % is rather small, the resulting shift in hardness value demonstrates that carbon is, by far, the most important alloying element when it comes to improving the material's hardness shown in Figure 10. Different carbides are formed depending on the quantity of carbon and chromium present, with more carbon and chromium concentration resulting in harder carbides. Carbide is also present in the microstructure of the hard-facing layer, and there are more of them when the alloying element content of the hard-facing layer is high.

3.3. Analysis of Erosive Wear

Since it has been shown that metals erode most rapidly at an angle of 30 degrees, that is where researchers focused their attention while studying the abrasive wear of the hard-faced layer. All samples were weighed before and after the experiment to provide an accurate reading. The results of the mass loss calculations for each sample are shown in Figure 11. It showed that the least amount of erosion occurred in the sample with the greatest quantity of alloying elements. This indicates that a hard-face layer with a higher proportion of carbides offers erosion resistance due to the material's increased hardness over the low-carbon steel used as a basis. The mass loss after the wear test is shown in Figure 11.

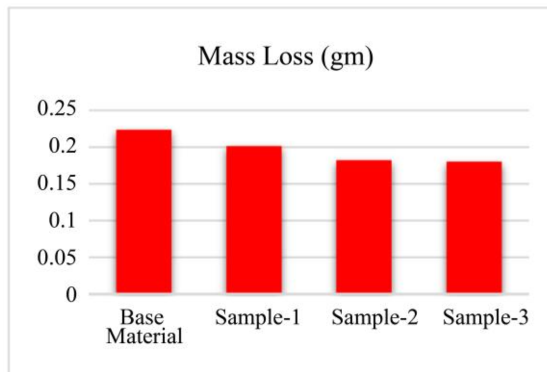

Fig. 11 Mass loss after wear test

3.4. Improvement in Hardness and Erosive Wear

Figure 12 shows the significant improvement in hardness as well as erosive wear resistance of sample-1, sample-2 and sample-3 when compared to the base material.

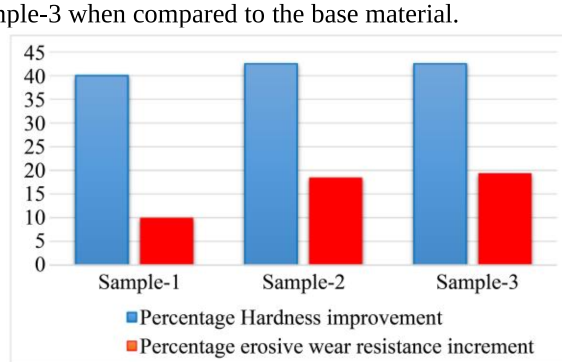

Fig. 12 Graphical representation of improved hardness and wear resistance in sample-1, sample-2 and sample-3

4. Conclusion

The following conclusions have been reached after completing the whole battery of tests, including all mechanical and metallurgical testing:

1. Iron based hard facing layer has been successfully developed with submerged arc welding process. Visual inspection of the final alloy shows defect defect-free hard facing layer.
2. The desired chemical composition in the hard-facing layer has been produced with the paste technique used in this process.
3. Hard-faced layer sample-2 and sample-3 have significant improvement in mechanical properties i.e. hardness of 142.5% as compared to base material.

Resistance to erosion has been increased in the hard facing layer as compared to the base material. There is also improvement in erosion resistance when carbide volume fraction is increasing in the alloy. Percentage erosive wear resistance increments 19.28 of sample-2 obtained.

Creating iron-based hard facing and studying its chemical and mechanical properties were within the purview of the current study. The effects of C and Cr element transfer behavior on related attributes were the primary focus of this research. The influence of additional alloying elements, such as Mn, Ni, Co, etc., on the hard-facing layer's characteristics would be an area of future research.

References

[1] L.E. Svensson et al., "Fe-Cr-C Hardfacing Alloys for High-Temperature Applications," *Journal of Materials Science*, vol. 21, pp. 1015-1019, 1986. [CrossRef] [Google Scholar] [Publisher Link]

[2] V.E. Buchanan, D.G. McCartney, and P.H. Shipway, "A Comparison of the Abrasive Wear Behaviour of Iron-Chromium Based Hardfaced Coatings Deposited by SMAW and Electric Arc Spraying," *Wear*, vol. 264, no. 7-8, pp. 542-549, 2008. [CrossRef] [Google Scholar] [Publisher Link]

[3] Vernon E. Buchanan, "Solidification and Microstructural Characterisation of Iron–Chromium Based Hardfaced Coatings Deposited by SMAW and Electric Arc Spraying," *Surface and Coatings Technology*, vol. 203, no. 23, pp. 3638-3646, 2009. [CrossRef] [Google Scholar] [Publisher Link]

[4] R. Choteborsky et al., "Abrasive Wear of High Chromium Fe-Cr-C Hardfacing Alloys," *Research in Agricultural Engineering*, vol. 54, no. 4, pp. 192-198, 2008. [CrossRef] [Google Scholar] [Publisher Link]

[5] Y.F. Zhou et al., "Fe–24 wt.%Cr–4.1 wt.%C Hardfacing Alloy: Microstructure and Carbide Refinement Mechanisms with Ceria Additive," *Materials Characterization*, vol. 72, pp. 77-86, 2012. [CrossRef] [Google Scholar] [Publisher Link]

[6] J. Hornung et al., "Influence of Cooling Speed on the Microstructure and Wear Behaviour of Hypereutectic Fe–Cr–C Hardfacings," *Materials Science and Engineering: A*, vol. 576, pp. 243-251, 2013. [CrossRef] [Google Scholar] [Publisher Link]

[7] Chia-Ming Chang, Yen-Chun Chen, and Weite Wu, "Microstructural and Abrasive Characteristics of High Carbon Fe–Cr–C Hardfacing Alloy," *Tribology International*, vol. 43, no. 5-6, pp. 929-934, 2010. [CrossRef] [Google Scholar] [Publisher Link]

[8] Jie-Hao Chen et al., "Microstructure and Abrasive Wear Properties of Fe-Cr-C Hardfacing Alloy Cladding Manufactured by Gas Tungsten Arc Welding (GTAW)," *Metals and Materials International*, vol. 19, pp. 93-98, 2013. [CrossRef] [Google Scholar] [Publisher Link]

[9] M. Morsy, and E. El-Kashif, "The Effect of Microstructure on High-Stress Abrasion Resistance of Fe-Cr-C Hardfacing Deposits," *Welding in the World*, vol. 58, pp. 491-497, 2014. [CrossRef] [Google Scholar] [Publisher Link]

[10] M. Kirchgaßner, E. Badisch, and F. Franek, "Behaviour of Iron-Based Hardfacing Alloys under Abrasion and Impact," *Wear*, vol. 265, no. 5-6, pp. 772-779, 2008. [CrossRef] [Google Scholar] [Publisher Link]

[11] Mustafa Sözeri et al., "Comparative Study of Hardfacing Applications on Structural Steel Surfaces to Improve Ballistic Properties," *Materials Today Communications*, vol. 38, 2024. [CrossRef] [Google Scholar] [Publisher Link]

[12] Nilay Çömez et al., "Fe-Cr-C-V Hardfacing Coatings with Molybdenum Addition: Wear, Corrosion, and Cavitation Performances," *Surface and Coatings Technology*, vol. 482, 2024. [CrossRef] [Google Scholar] [Publisher Link]

[13] Dashuang Liu et al., "Effect of Mo on Microstructure and Wear Resistance of Slag-Free Self-Shielded Metal-Cored Welding Overlay," *Journal of Materials Processing Technology*, vol. 270, pp. 82-91, 2019. [CrossRef] [Google Scholar] [Publisher Link]

[14] Jingli Zhang et al., "Microstructure and Abrasive Wear Resistance Evolution of Water and Liquid Nitrogen Forced Cooling Fe-Cr-C Deposit," *Tribology International*, vol. 174, 2022. [CrossRef] [Google Scholar] [Publisher Link]

[15] Jibo Wang et al., "Effect of Nitrogen Alloying on the Microstructure and Abrasive Impact Wear Resistance of Fe-Cr-C-Ti-Nb Hardfacing Alloy," *Surface and Coatings Technology*, vol. 309, pp. 1072-1080, 2017. [CrossRef] [Google Scholar] [Publisher Link]

[16] H. Rojacz et al., "Impact-Abrasive Wear of Martensitic Steels and Complex Iron-Based Hardfacing Alloys," *Wear*, vol. 492-493, 2022. [CrossRef] [Google Scholar] [Publisher Link]

[17] Ramin Zahiri et al., "Hardfacing Using Ferro-Alloy Powder Mixtures by Submerged Arc Welding," *Surface and Coatings Technology*, vol. 260, pp. 220-229, 2014. [CrossRef] [Google Scholar] [Publisher Link]

[18] E. Badisch et al., "Wear Behaviour of Hardfaced Fe-Cr-C Alloy and Austenitic Steel under 2-Body and 3-Body Conditions at Elevated Temperature," *Tribology International*, vol. 43, no. 7, pp. 1234-1244, 2010. [CrossRef] [Google Scholar] [Publisher Link]

[19] C. Katsich et al., "Erosive Wear of Hardfaced Fe–Cr–C Alloys at Elevated Temperature," *Wear*, vol. 267, no. 11, pp. 1856-1864, 2009. [CrossRef] [Google Scholar] [Publisher Link]

[20] Ricardo Vinicius de Melo Leite, and Paulo Villani Marques, "Comparative Study of the Wear Resistance of Three Metal-Fluxed Core Wire-Welded Coatings Used in Industry," *Welding International*, vol. 25, no. 12, pp. 917-922, 2011. [CrossRef] [Google Scholar] [Publisher Link]

[21] Chayanee Tippayasam et al., "Effects of Flux-Cored Arc Welding Technology on Microstructure and Wear Resistance of Fe-Cr-C Hardfacing Alloy," *Materials Today Communications*, vol. 35, 2023. [CrossRef] [Google Scholar] [Publisher Link]

[22] Aleksandra Świerczyńska et al., "Exploring the Trends in Flux-Cored Arc Welding: Scientometric Analysis Approach," *The International Journal of Advanced Manufacturing Technology*, vol. 130, no. 1, pp. 87-110, 2024. [CrossRef] [Google Scholar] [Publisher Link]

[23] Qicong Liu et al., "Effect of Different Chromium Contents on Microstructure and Two-Body Abrasive Wear Behavior of Fe-Mn-B Surfacing Alloys," *Materials Today Communications*, vol. 36, 2023. [CrossRef] [Google Scholar] [Publisher Link]